Journal of Hazardous Materials Letters 6 (2025) 100148

Contents lists available at ScienceDirect

Journal of Hazardous Materials Letters

journal homepage: www.sciencedirect.com/journal/journal-of-hazardous-materials-letters

Recovery of nitrate and fluoride salts from stainless steel pickling wastewater with flow-electrode capacitive deionization

Niklas Köller [a], Dustin Roedder [a], Christian J. Linnartz [a,b], Mark Enders [c], Florian Morell [d], Patrick Altmeier [e], Matthias Wessling [a,b,*]

[a] RWTH Aachen University, Aachener Verfahrenstechnik-Chemical Process Engineering, Forckenbeckstraße 51, Aachen 52074, Germany
[b] DWI - Leibniz Institute for Interactive Materials e.V., Forckenbeckstraße 50, Aachen 52074, Germany
[c] SIMA-tec GmbH, Schier 12c, Schwalmtal 41366, Germany
[d] Outokumpu Nirosta GmbH, Oberschlesienstraße 16, Krefeld 47807, Germany
[e] PCCell GmbH, Lebacher Straße 60, Heusweiler 66265, Germany

ARTICLE INFO

Keywords:
Flow-electrode capacitive deionization
Stainless steel pickling
Salt brines
Nitrate
Fluoride

ABSTRACT

Flow-electrode Capacitive Deionization (FCDI) is an innovative method for practical salt removal and recycling applications. Here, we report that FCDI facilitates the recovery of nitrate and fluoride salts from brines produced during the wastewater treatment process in a stainless steel pickling line. Laboratory-scale experiments with synthetic wastewaters were used to evaluate the influence of (a) the membrane thickness, (b) feed flow rates, and (c) applied voltage on the outlet concentrations and the average salt transfer rate. In continuous single-pass experiments, the flow rates of diluate and concentrate have the greatest influence on the resulting outlet concentrations in the FCDI process as they directly influence the residence time. The operating voltage of the FCDI process can be varied to increase the ratio of fluoride over nitrate for recycling.

1. Introduction

Stainless steel is a large-scale commodity product with a wide variety of applications. During production, stainless steel is handled at elevated temperatures (e.g., during casting or annealing). This causes the formation of an oxide scale layer and a chromium-depleted layer at the surface. These layers not only impair the optical properties of the surface but also reduce corrosion resistance. Steel pickling achieves the desired qualities by removing the surface layers and exposing the metal beneath (Covino et al., 1984; Li & Celis, 2003). An important part of the pickling process is chemical pickling in acid baths. Hydrofluoric acid (HF) and nitric acid (HNO_3) are often used in these pickling baths (Li et al., 2005). During pickling, the dissolved metal concentrations in the acid solutions increase, lowering the efficiency of the pickling process. Recovery of dissolved metals and acid solutions from spent pickling solutions is motivated by environmental regulations and economic benefits (Regel-Rosocka, 2010). Different recovery methods discussed in the literature include precipitation, evaporation, vacuum distillation, crystallization, spray roasting, ion exchange, solvent extraction, and various membrane processes (Regel-Rosocka, 2010; Agrawal & Sahu, 2009; Leonzio, 2016; Devi et al., 2014; McCabe & Vivona, 1999; Hsu et al., 2023). Notably, Negro et al. suggested a combination of Electrodialysis (ED) and ED with bipolar membranes (EDBM) for the concentration and splitting of salt solutions after the neutralization of the spent acids (Negro et al., 2001). Their work used Diffusion Dialysis (DD) to recycle the free acids. The remaining acids were neutralized with potassium hydroxide (KOH) to obtain highly soluble potassium nitrate (KNO_3) and potassium fluoride (KF) in solution. Subsequently, EDBM was used to produce the acids and KOH; ED was proposed to increase the concentration of wash water with low acid concentrations before the EDBM step (Negro et al., 2001). However, the concentration step was not investigated in their work, the main focus was on the EDBM step.

Inspired by their work, we suggest a simplified treatment process in which the ED concentration step is replaced by Flow-electrode Capacitive Deionization (FCDI), enabling the recycling of both HNO_3 and HF in high concentrations. Fig. 1 (a) shows the proposed flow chart of the process. In the present work, we focus in detail on the concentration step with FCDI, which is critical to providing high concentrations to the subsequent EDBM step. The ion transport in the FCDI process used in the experiments is detailed in Fig. 1 (b).

* Corresponding author at: RWTH Aachen University, Aachener Verfahrenstechnik-Chemical Process Engineering, Forckenbeckstraße 51, Aachen 52074, Germany.
E-mail address: manuscripts.cvt@avt.rwth-aachen.de (M. Wessling).

https://doi.org/10.1016/j.hazl.2025.100148
Received 10 October 2024; Received in revised form 6 February 2025; Accepted 18 February 2025
Available online 20 February 2025

Investigations of the FCDI process in literature show an energy demand comparable to ED while reaching a high water recovery and avoiding the formation of by-product gases, which could pose safety risks (e.g., hydrogen) (Rommerskirchen et al., 2020). FCDI uses the principle of capacitive ion adsorption and desorption at a charged surface. The required surface area is provided by conductive particles (often activated carbon) in the flow electrode (Folaranmi et al., 2022). Ions migrate in the electrical field and adsorb to the particles. The particles are continuously pumped to a second channel in the FCDI module, where desorption and regeneration of the particles occur (Rommerskirchen et al., 2015). Due to the primarily electrosorptive process, electrochemical faradaic reactions at the electrodes can be avoided (Porada et al., 2013; Shin et al., 2021). The principle is illustrated in Fig. 1 (b). FCDI was investigated for treating groundwaters and brackish waters containing nitrate and fluoride salts, showing the technology's applicability (Song et al., 2019; Sun et al., 2023; Jiang et al., 2022).

In this work, the application of FCDI to a synthetic solution of KNO_3 and KF is tested in laboratory experiments. The transfer of the results to a pilot plant is planned for future investigation. The feed concentrations are based on brine concentrations measured after acid neutralization with KOH at the stainless steel pickling plant of Outokumpu Nirosta GmbH in Dillenburg, Germany. The present study aims to highlight the engineering process needed to tailor the FCDI process to this specific salt recycling task.

2. Materials and methods

Experiments were conducted with an FCDI single module with a total membrane area $A_{mem,tot}$= 300 cm^2 (Rommerskirchen et al., 2015) and the flow electrode in short-circuited closed cycle (SCC) operation. Graphite current collectors (180 mm × 180 mm × 10 mm, Müller & Rössner GmbH & Co. KG) were used. Flow-electrode channels with 18 turns (3 mm × 2 mm and 2000 mm total length) were milled into the current collectors. Membrane spacers (ED-100, thickness 500 μm, Fumatech BWT GmbH) formed the concentrate and diluate channels between ion-exchange membranes. One cation-exchange membrane (Fumasep FKS, 75 μm PET-reinforced, Fumatech BWT GmbH) was placed adjacent to each current collector. An AEM (Fumasep FAS, 75 μm PET-reinforced, Fumatech BWT GmbH) separated the two flow channels. Conductivity probes were used to measure the conductivity of the outgoing diluate (SE 615/1-MS, Knick Elektronische Messgeräte GmbH Co. KG) and concentrate (LTC 0,35/23, Xylem Analytics Germany Sales GmbH & Co. KG).

The experiments were carried out in continuous single-pass operation. The conductivities at the outlets developed to a steady state. When a steady state was reached, samples were collected for evaluation with ion chromatography (930 Compact IC Flex, Deutsche METROHM GmbH & Co. KG. Anion column: Metrosep A Supp 7–250/4.0. Cation column: Metrosep C 6–250/4.0).

The concentrations of synthetic wastewater were based on samples from small-scale neutralization. The diluate feed solution consisted of 38.03 g L^{-1} KNO_3 (Potassium Nitrate 99 %, Carl Roth GmbH + Co. KG) and 33.38 g L^{-1} KF (Potassium Fluoride 99 %, Carl Roth GmbH + Co. KG). These concentrations are lower than typical concentrations in spent pickling solutions from literature due to the preceding acid recovery step, shown in Fig. 1 (a). Thus, the concentrations are unique to the specific use case. Higher concentrations were used for the concentrate feed solution (83.67 g L^{-1} KNO_3 and 73.44 g L^{-1} KF). These concentrations are expected in the loop between EDBM and FCDI in the

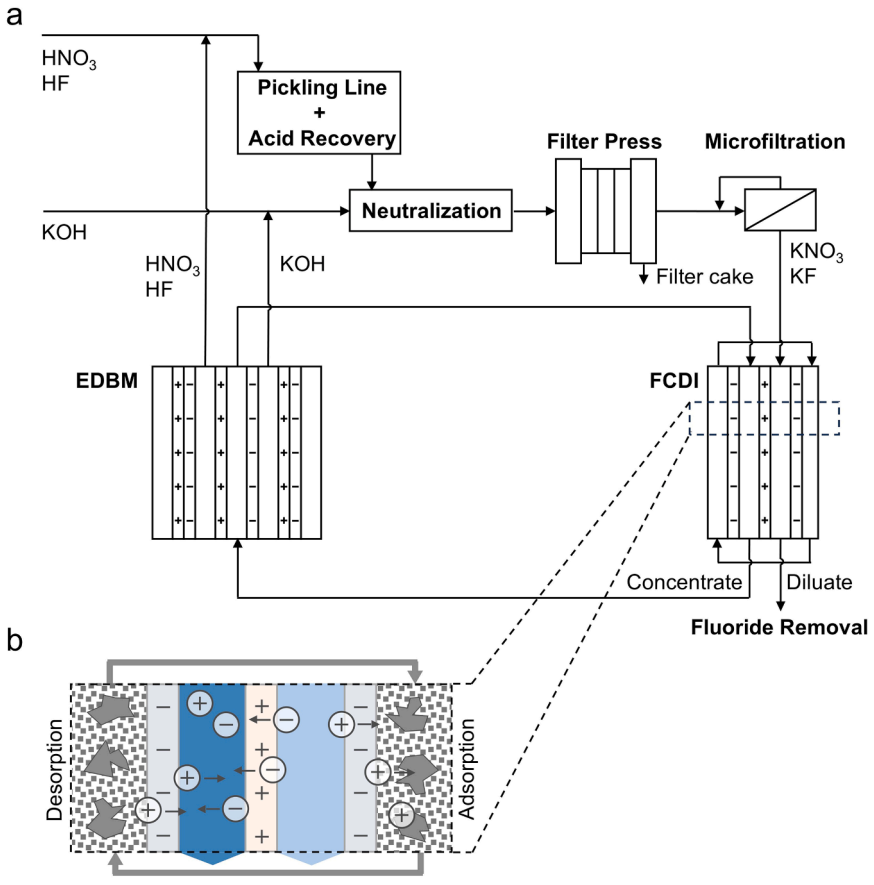

Fig. 1. Proposed process for the recycling of HF and HNO_3 from pickling line wastewater. (a): Flow chart showing the process. The flow chart does not include chromium detoxification and filter cake post-treatment. (b): Ion transport processes occurring in the FCDI process.

proposed process. Flow electrodes were prepared by suspending 15 *wt.* % activated carbon powder (Carbopal SC11PG, Donau Carbon GmbH) in salt solutions with varying concentrations of KNO_3 and KF.

The metrics used to evaluate the results are the changes in concentration for diluate and concentrate (c_D/c_{FD} and c_C/c_{FC}), and the average salt transfer rate (ASTR) given in Eq. (1) and Eq. (2). The energy demand per treated diluate E_D given in Eq. (3) allows a first evaluation of the electrical energy demand of the process.

$$ASTR_i = \frac{\Delta \dot{m}_i}{A_{mem,tot} \cdot M_i} \tag{1}$$

$$ASTR_{tot} = \sum_i ASTR_i \tag{2}$$

$$E_D = \frac{V \cdot I}{\dot{V}_{FD}} \tag{3}$$

3. Results and discussion

3.1. Electrolyte concentration in flow electrode

The flow electrode used in the FCDI process typically contains an electrolyte to increase its conductivity (Zhang et al., 2021). Ideally, the flow electrode should be in osmotic equilibrium with the neighboring channels so that the water content in the flow electrode remains constant over time. This is impossible to achieve prior to steady state, as the flow electrode is in contact with both diluate and concentrate, which establish different concentrations in steady state. In the long-term operation of an FCDI process, water loss from the flow electrode is easier to control. Lost water can be added to the flow electrode by a dosing pump. Thus, the goal is a background electrolyte concentration that causes a minimum amount of water loss. Results from an investigation of different electrolyte concentrations in the flow electrode are given in the `Supplementary Information`. To minimize the use of toxic KF in the process, a flow electrode with only KNO_3 is selected. The concentration is $c_{FE,KNO_3} = 149.64\ g\ L^{-1}$.

3.2. Membrane thickness

The transport of ions and water in electro-membrane processes are strongly influenced by the properties of ion-exchange membranes (Porada et al., 2018). Here, the influence of membrane thickness on the FCDI process is of particular importance, as it can influence the water crossover. The middle membrane that separates the diluate and concentrate compartments was changed from a $d_{AEM} = 75\mu m$ thick FAS-PET-75 membrane to a $d_{AEM} = 130\mu m$ thick FAS-PET-130 membrane. The hypothesis of the central membrane affecting osmotic water transport is based on the fact that the concentration gradient between the diluate and concentrate is more significant than that between each channel and the adjacent flow electrode channel.

The experiments were carried out with a constant current of $I = 1.6$ A. In constant current operation, the ion transport is equal in both experiments. Therefore, changes in the outlet concentrations can be attributed to water transport. The diluate feed flow rate was set to $\dot{V}_{FD} = 1.18\ mL\ min^{-1}$ and the concentrate feed flow rate to $\dot{V}_{FC} = 0.50\ mL\ min^{-1}$. Fig. 2 (a) shows the ASTR with a membrane thickness of $d_{AEM} = 75\mu m$ and $d_{AEM} = 130\mu m$. $ASTR_{tot}$ and the individual $ASTR_{KNO_3}$ and $ASTR_{KF}$ are not influenced by d_{AEM}. However, water transport differs. The right y-axis shows the quotient of salt transport and water transport: this metric increases from 0.29 mg_{Salt}/mg_{H_2O} to 0.34 mg_{Salt}/mg_{H_2O} for the thicker membrane. Since the salt transport (given by the ASTR) remains constant, this signifies reduced water transport across the middle membrane. Fig. 2 (b) shows the effect on the concentrations of diluate and concentrate at the module outlet. The concentration difference of KNO_3 and KF increases slightly.

The electrical energy demand per cubic meter of treated diluate can be calculated according to Eq. (3). This metric does not include any additional energy (e.g., energy of the pumps in the experiment). The energy demand rises from 48.0 kWh/m^3_D for $d_{AEM} = 75\mu m$ to 55 kWh/m^3_D for $d_{AEM} = 130\mu m$. Thus, 13 % of electrical energy can be saved by using thinner membranes. Because the effect of increased water transport on outlet concentrations was low in comparison, experiments were continued with FAS-75 membranes with $d_{AEM} = 75\mu m$.

3.3. Feed flow rate

In continuous single-pass experiments, outlet concentrations are influenced by diluate and concentrate feed flow rates ($\dot{V}_{FD}$ and $\dot{V}_{FC}$). Lower flow rates lead to longer residence times of the fluids in the electric field, leading to higher concentration differences between the inlet and outlet. The diluate and concentrate channels influence each other due to the transfer of ions and water. First, $\dot{V}_{FD}$ was varied, while $\dot{V}_{FC}$ was kept constant. In a second step, $\dot{V}_{FC}$ was varied while $\dot{V}_{FD}$ was kept constant.

Fig. 3 (a) shows constant KNO_3 diluate concentration ($c_{D,KNO_3}/c_{FD,KNO_3}$) throughout the investigated range of $\dot{V}_{FD}$. Even at the highest $\dot{V}_{FD}$ most KNO_3 is removed from the diluate feed. $c_{D,KF}/c_{FD,KF}$ increases with an increase in the diluate flow rate due to lower residence time. On the concentrate side $c_{C,KNO_3}/c_{FC,KNO_3}$ and $c_{C,KF}/c_{FC,KF}$ both increase. Thus, the optimal diluate feed flow rate is as high as possible but low enough to achieve the desired outlet concentrations. The required

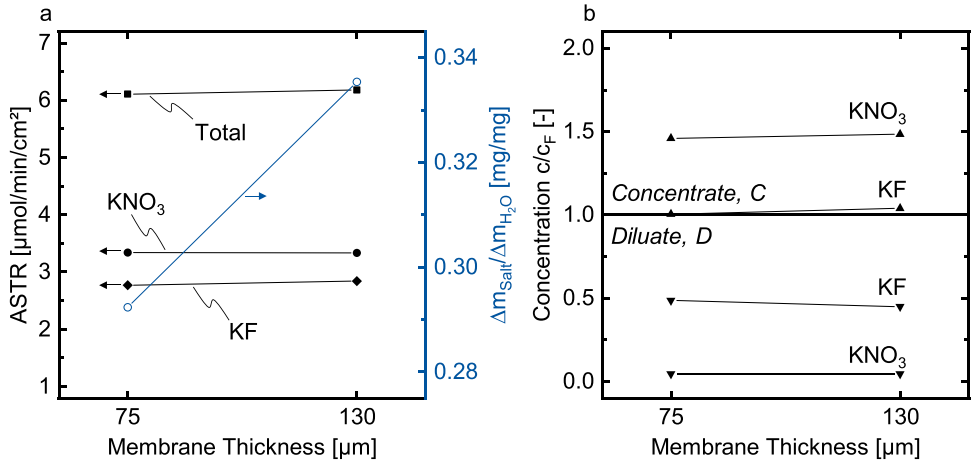

Fig. 2. Influence of the thickness of the middle AEM on the salt and water transport in the FCDI module. Data points are connected by lines to guide the reader's eye.

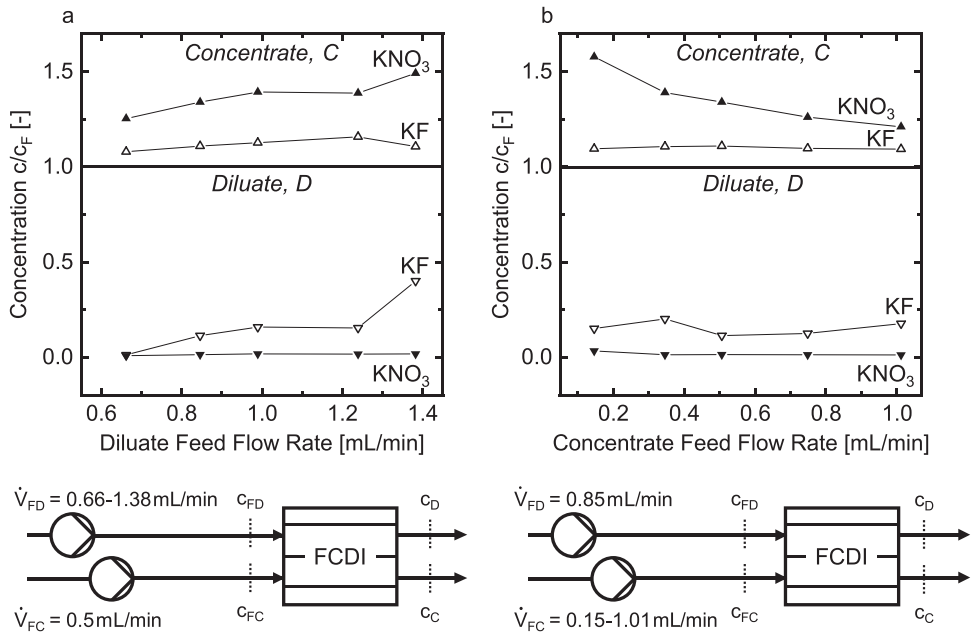

Fig. 3. (a): Effect of the variation of the diluate feed flow rate on the outlet concentrations. (b): Effect of the variation of the concentrate feed flow rate on the outlet concentrations. Data points are connected by lines to guide the reader's eye.

outlet concentration for the application is $0.1 \cdot c_{FD}$. Thus, a viable diluate feed flow rate can be found at $\dot{V}_{FD} = 0.85$ mL min^{-1}.

In the second step, $\dot{V}_{FD} = 0.85$ mL min^{-1} was kept constant, and $\dot{V}_{FC}$ was varied to increase the outlet concentrations as shown in Fig. 3 (b). Generally, the influence of $\dot{V}_{FC}$ on the diluate concentrations is low. At $\dot{V}_{FC} = 0.15$ mL min^{-1} the concentration degree of KNO_3 is highest at $c_{C,KNO_3} = 1.58 \cdot c_{FC,KNO_3}$. An increase in $\dot{V}_{FC}$ leads to a decrease in concentration. The lowest concentration is $c_{C,KNO_3} = 1.21 \cdot c_{FC,KNO_3}$ at $\dot{V}_{FC} = 1.01$ mL min^{-1}. The concentration of KF is not influenced by $\dot{V}_{FC}$ as much, since it only varies between $1.09 \cdot c_{FC,KF}$ and $1.11 \cdot c_{FC,KF}$. Overall, $\dot{V}_{FC}$ mainly influences the concentration degree of KNO_3 while the concentration degree of KF remains almost constant. This can be explained with the preferential transport of nitrate over the AEM (Sata, 2000; Luo et al., 2018).

In summary, the target concentration of $0.1 \cdot c_{FD}$ on the diluate side can be reached for both salts. On the concentrate side, a targeted degree of concentration of $1.3 \cdot c_{FC}$ can only be reached for KNO_3. To improve the concentration degree of KF, operation with increased voltages is tested.

3.4. Operating voltage

Typically, FCDI processes are operated with a voltage of 1.2 V. This ensures that no faradaic reactions can occur, since the standard potential difference for water electrolysis is 1.23 V (Shin et al., 2021). However, there is also literature on FCDI processes at higher voltages (Tang et al., 2020; Xu et al., 2017). Higher voltages lead to a higher driving force for ion transport. The hypothesis for this investigation was that higher voltages can improve the concentration differences found in the investigation of flow rates in Section 3.3. Here, voltages up to 2.0 V were investigated.

Since almost all KNO_3 is already transported from the diluate when operating with 1.2 V, no increase in KNO_3 transport is expected. The goal of the experiments is to increase the transport of KF to reach lower concentrations in the diluate and higher concentrations in the concentrate. The feed flow rates are fixed at $\dot{V}_{FD} = 1.35$ mL min^{-1} and $\dot{V}_{FC} = 0.53$ mL min^{-1}. The current efficiencies (calculated for the steady state of experiments according to (Zhang et al., 2021)) in all experiments are above 90 %, indicating that the extent of water splitting at the electrodes is low.

Fig. 4 (a) shows the ASTRs for KF and KNO_3 and the total ASTR for increased voltages. The ASTR for KNO_3 remains constant, the ASTR for KF increases from 3.34 μmol min^{-1} cm^{-2} at 1.2 V to 4.92 μmol min^{-1} cm^{-2} at 2.0 V. The increased ion transport at elevated voltages also causes changes to the water transport between diluate and concentrate: the additionally transported fluoride and potassium ions lead to more water transport from the diluate to the concentrate. A more detailed analysis of water transport is given in the `Supplementary Information`.

This water transport also impacts both salts' outlet concentrations c_D and c_C. Fig. 4 (b) shows that the diluate concentration of KNO_3 remains constant at very low values (between 4 % and 1 % of the feed concentration). The KF concentration decreases from $0.48 \cdot c_{F,KF}$ at 1.2 V to $0.09 \cdot c_{F,KF}$ at 2.0 V. Thus, lower KF outlet concentrations can be reached with elevated voltages. However, the concentrate side also needs to be taken into account. Here, the KF concentration increases from $1.07 \cdot c_{F,KF}$ to $1.17 \cdot c_{F,KF}$. However, as shown in Fig. 4 (b), the increased KF transport also causes increased water transport from the diluate into the concentrate. No more KNO_3 could be transported to balance the increased water transport, and the outlet concentration c_{C,KNO_3} decreases at higher voltages. At 1.2 V the outlet concentration is $c_{C,KNO_3} = 1.51 \cdot c_{F,KNO_3}$; at 2.0 V it is only $c_{C,KNO_3} = 1.39 \cdot c_{F,KNO_3}$. Therefore, a trade-off exists between a higher concentration of KF at high voltages and a high concentration of KNO_3 at low voltages. Additionally, elevated voltages cause an increase in electrical energy demand from 27.1 kWh/m^3_D at 1.2 V to 56.5 kWh/m^3_D at 2.0 V. Tailoring of KNO_3 and KF concentrations by variation of the voltage needs to be further studied in the proposed salt recycling process together with the EDBM step.

4. Conclusion and outlook

FCDI is an emerging process for the simultaneous desalination and the concentration of salt brines from industry processes. For the first time FCDI was used to concentrate nitrate and fluoride-containing wastewaters from stainless steel pickling. The target on the diluate side was a reduction of the concentration to at least 10 % of the feed concentration; on the concentrate side the concentrations should be

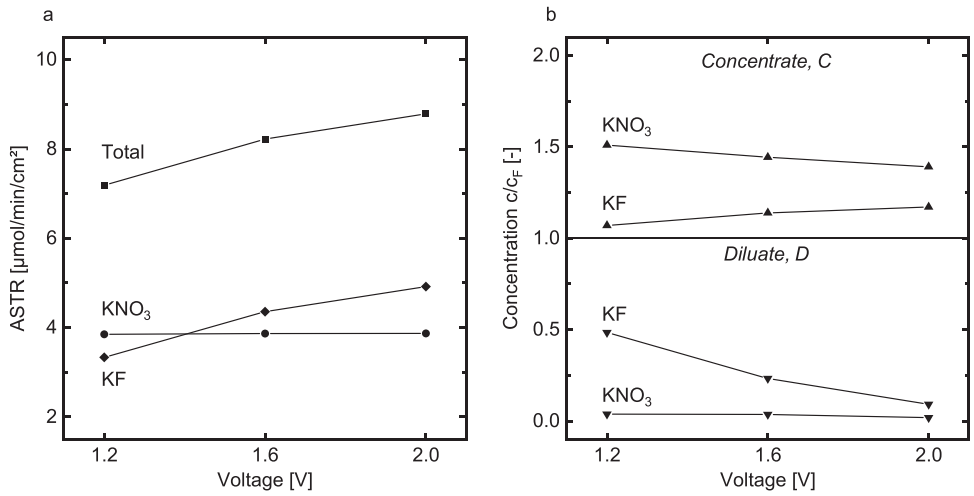

Fig. 4. Effect of operating voltage on (a) ASTR and (b) water transport. Data points are connected by lines to guide the reader's eye.

increased to 130 %, to enable salt recycling with EDBM in the next step. In the lab-scale experiments synthetic wastewaters were used and the influence of (a) the membrane thickness, (b) the feed flow rates, and (c) the applied voltage was investigated. Operation with a well-adjusted electrolyte concentration in the flow electrode is important to avoid high water crossover between the flow electrode and the diluate/concentrate. In continuous single-pass experiments, the flow rates of diluate and concentrate have the greatest influence on the resulting outlet concentrations and can be used to tune the FCDI process. While the target concentrations on the diluate side were reached, it was not possible to reach high potassium fluoride concentrations on the concentrate side. Increased voltages offer no solution in the specific case since the increased transport of potassium fluoride at higher voltages causes more water transport, lowering the potassium nitrate concentration.

In future research on the salt recycling process introduced here, the recycle loop between FCDI and EDBM must be closed. Furthermore, results from lab scale need to be transferred to pilot scale. To enable this, onsite tests with wastewater at the stainless steel treatment plant are necessary.

Funding information

This work was supported by the German Federal Ministry of Education and Research (BMBF) under the project "NITREB" (FKZ 02WQ1534D). M.W. acknowledges DFG funding through the Gottfried Wilhelm Leibniz Award 2019, Germany (WE 4678/12–1). M. W. appreciates the support from the Alexander-von-Humboldt foundation.

CRediT authorship contribution statement

Mark Enders: Writing – review & editing, Funding acquisition, Conceptualization. **Christian Jürgen Linnartz:** Writing – review & editing, Writing – original draft, Visualization, Validation, Supervision, Project administration, Methodology, Funding acquisition, Formal analysis, Data curation, Conceptualization. **Patrick Altmeier:** Funding acquisition, Conceptualization. **Florian Morell:** Writing – review & editing, Funding acquisition, Conceptualization. **Matthias Wessling:** Writing – review & editing, Writing – original draft, Visualization, Supervision, Resources, Project administration, Methodology, Funding acquisition, Conceptualization. **Dustin Roedder:** Visualization, Investigation, Data curation. **Niklas Köller:** Writing – review & editing, Writing – original draft, Visualization, Validation, Supervision, Project administration, Methodology, Investigation, Formal analysis, Data curation, Conceptualization.

Declaration of Competing Interest

The authors declare the following financial interests/personal relationships which may be considered as potential competing interests: Matthias Wessling reports financial support was provided by Federal Ministry of Education and Research Berlin Office. Matthias Wessling reports financial support was provided by German Research Foundation. Matthias Wessling has patent Apparatus and method for continuous water desalination and ion separation by flow electrode capacitive deionization issued to DWI - Leibniz-Institut für Interaktive Materialien e.V. Matthias Wessling, Christian Linnartz has patent Electrochemical Module Comprising a Flexible Membrane-Electrode Assembly issued to DWI - Leibniz-Institut für Interaktive Materialien e.V. If there are other authors, they declare that they have no known competing financial interests or personal relationships that could have appeared to influence the work reported in this paper.

Data availability

Data will be made available on request.

Acknowledgments

The authors thank Timo Linzenmeier for IC measurements.

Appendix A. Supporting information

Supplementary data associated with this article can be found in the online version at doi:10.1016/j.hazl.2025.100148.

References

Agrawal, A., Sahu, K., 2009. An overview of the recovery of acid from spent acidic solutions from steel and electroplating industries. J. Hazard. Mater. 171 (1), 61–75. https://doi.org/10.1016/j.jhazmat.2009.06.099.

B.S. Covino, J.V. Scalera, P.M. Fabis, Pickling of stainless steels–a review, US Department of the Interior, Bureau of Mines (1984). archive.org/details/picklingofstainl00covi.

Devi, A., Singhal, A., Gupta, R., Panzade, P., 2014. A study on treatment methods of spent pickling liquor generated by pickling process of steel. Clean. Technol. Environ. Policy 16, 1515–1527. https://doi.org/10.1007/s10098-014-0726-7.

Folaranmi, G., Tauk, M., Bechelany, M., Sistat, P., Cretin, M., Zaviska, F., 2022. Investigation of fine activated carbon as a viable flow electrode in capacitive deionization. Desalination 525, 115500. https://doi.org/10.1016/j.desal.2021.115500.

Hsu, C.-J., Xiao, Y.-Z., Chung, A., Hsi, H.-C., 2023. Novel applications of vacuum distillation for heavy metals removal from wastewater, copper nitrate hydroxide recovery, and copper sulfide impregnated activated carbon synthesis for gaseous mercury adsorption. Sci. Total Environ. 855, 158870. https://doi.org/10.1016/j.scitotenv.2022.158870.

Jiang, H., Zhang, J., Luo, K., Xing, W., Du, J., Dong, Y., Li, X., Tang, W., 2022. Effective fluoride removal from brackish groundwaters by flow-electrode capacitive deionization (FCDI) under a continuous-flow mode. Sci. Total Environ. 804, 150166. https://doi.org/10.1016/j.scitotenv.2021.150166.

Leonzio, G., 2016. Recovery of metal sulphates and hydrochloric acid from spent pickling liquors. J. Clean. Prod. 129, 417–426. https://doi.org/10.1016/j.jclepro.2016.04.037.

Li, L.-F., Celis, J.-P., 2003. Pickling of austenitic stainless steels (a review). Can. Metall. Q 42 (3), 365–376. https://doi.org/10.1179/cmq.2003.42.3.365.

Li, L.-F., Caenen, P., Daerden, M., Vaes, D., Meers, G., Dhondt, C., Celis, J.-P., 2005. Mechanism of single and multiple step pickling of 304 stainless steel in acid electrolytes. Corros. Sci. 47 (5), 1307–1324. https://doi.org/10.1016/j.corsci.2004.06.025.

Luo, T., Abdu, S., Wessling, M., 2018. Selectivity of ion exchange membranes: A review. J. Membr. Sci. 555, 429–454. https://doi.org/10.1016/j.memsci.2018.03.051.

McCabe, D.L., Vivona, M.A.T., 1999. Treating process wastewater employing vacuum distillation using mechanical vapor recompression. Environ. Prog. 18 (1), 30–33. https://doi.org/10.1002/ep.670180117.

Negro, C., Blanco, M.A., López-Mateos, F., DeJong, A.M.C.P., LaCalle, G., Erkel, J.V., Schmal, D., 2001. Free acids and chemicals recovery from stainless steel pickling baths. Sep. Sci. Technol. 36 (7), 1543–1556. https://doi.org/10.1081/SS-100103887.

Porada, S., Zhao, R., van der Wal, A., Presser, V., Biesheuvel, P.M., 2013. Review on the science and technology of water desalination by capacitive deionization. Prog. Mater. Sci. 58 (8), 1388–1442. https://doi.org/10.1016/j.pmatsci.2013.03.005.

Porada, S., van Egmond, W., Post, J., Saakes, M., Hamelers, H., 2018. Tailoring ion exchange membranes to enable low osmotic water transport and energy efficient electrodialysis. J. Membr. Sci. 552, 22–30. https://doi.org/10.1016/j.memsci.2018.01.050.

Regel-Rosocka, M., 2010. A review on methods of regeneration of spent pickling solutions from steel processing. J. Hazard. Mater. 177 (1), 57–69. https://doi.org/10.1016/j.jhazmat.2009.12.043.

Rommerskirchen, A., Gendel, Y., Wessling, M., 2015. Single module flow-electrode capacitive deionization for continuous water desalination. Electrochem. Commun. 60, 34–37. https://doi.org/10.1016/j.elecom.2015.07.018.

Rommerskirchen, A., Linnartz, C.J., Egidi, F., Kendir, S., Wessling, M., 2020. Flow-electrode capacitive deionization enables continuous and energy-efficient brine concentration. Desalination 490, 114453. https://doi.org/10.1016/j.desal.2020.114453.

Sata, T., 2000. Studies on anion exchange membranes having permselectivity for specific anions in electrodialysis — effect of hydrophilicity of anion exchange membranes on permselectivity of anions. J. Membr. Sci. 167 (1), 1–31. https://doi.org/10.1016/S0376-7388(99)00277-X.

Shin, Y.-U., Lim, J., Boo, C., Hong, S., 2021. Improving the feasibility and applicability of flow-electrode capacitive deionization (FCDI): review of process optimization and energy efficiency. Desalination 502, 114930. https://doi.org/10.1016/j.desal.2021.114930.

Song, J., Ma, J., Zhang, C., He, C., Waite, T.D., 2019. Implication of non-electrostatic contribution to deionization in flow-electrode cdi: case study of nitrate removal from contaminated source waters. Front. Chem. 7. https://doi.org/10.3389/fchem.2019.00146.

Sun, J., Garg, S., Waite, T.D., 2023. A novel integrated flow-electrode capacitive deionization and flow cathode system for nitrate removal and ammonia generation from simulated groundwater. Environ. Sci. Technol. 57, 14726–14736. https://doi.org/10.1021/acs.est.3c03922.

Tang, K., Yiacoumi, S., Li, Y., Gabitto, J., Tsouris, C., 2020. Optimal conditions for efficient flow-electrode capacitive deionization. Sep. Purif. Technol. 240, 116626. https://doi.org/10.1016/j.seppur.2020.116626.

Xu, X., Wang, M., Liu, Y., Lu, T., Pan, L., 2017. Ultrahigh desalinization performance of asymmetric flow-electrode capacitive deionization device with an improved operation voltage of 1.8 V. ACS Sustain. Chem. Eng. 5 (1), 189–195. https://doi.org/10.1021/acssuschemeng.6b01212.

Zhang, C., Ma, J., Wu, L., Sun, J., Wang, L., Li, T., Waite, T.D., 2021. Flow electrode capacitive deionization (FCDI): recent developments, environmental applications, and future perspectives. Environ. Sci. Technol. 55, 4243–4267. https://doi.org/10.1021/acs.est.0c06552.